AD-A063 097 CALIFORNIA UNIV IRVINE DEPT OF PHYSICS F/G 20/12
THEORY OF SURFACE POLARITONS IN N-TYPE SILICON IN THE PRESENCE --ETC(U)
DEC 78 B G MARTIN, A A MARADUDIN, R F WALLIS N00014-76-C-0121
UNCLASSIFIED TR-78-51 NL

| OF |
AD
A063097

END
DATE
FILMED
3-79
DDC

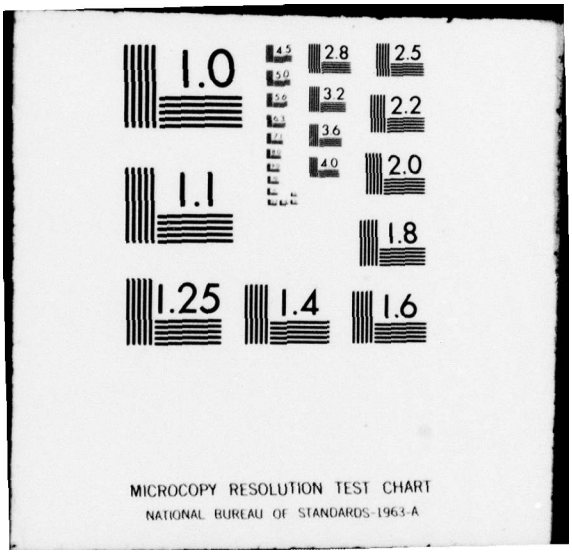
1.0
1.1
1.25
2.8
3.2
3.6
4.0
2.5
2.2
2.0
1.8
1.4
1.6
MICROCOPY RESOLUTION TEST CHART
NATIONAL BUREAU OF STANDARDS-1963-A

SECURITY CLASSIFICATION OF THIS PAGE (When Data Entered)

REPORT DOCUMENTATION PAGE

(13) LEVEL II

1. REPORT NUMBER	2. GOVT ACCESSION NO.	READ INSTRUCTIONS BEFORE COMPLETING FORM RECIPIENT'S CATALOG NUMBER

4. TITLE (and Subtitle)
(6) Theory of Surface Polaritons in n-Type Silicon in the Presence of a DC Current.
(10)

5. TYPE OF REPORT & PERIOD COVERED
(9) FINAL rept.

6. PERFORMING ORG. REPORT NUMBER
(14) TR-78-51

7. AUTHOR(s)
B. G. Martin, A. A. Maradudin and R. F. Wallis

8. CONTRACT OR GRANT NUMBER(s)
ONR N00014-76-C-0121
(15)

9. PERFORMING ORGANIZATION NAME AND ADDRESS
University of California, Irvine
Irvine, CA 92717

10. PROGRAM ELEMENT, PROJECT, TASK AREA & WORK UNIT NUMBERS
NR 392-00.
(11)

11. CONTROLLING OFFICE NAME AND ADDRESS
Office of Naval Research, Physics Program
800 N. Quincy St., Arlington, VA 22217

12. REPORT DATE
DECEMBER 1978

13. NUMBER OF PAGES
26

14. MONITORING AGENCY NAME & ADDRESS(if different from Controlling Office)
(12) 27p.

15. SECURITY CLASS. (of this report)
UNCLASSIFIED

15a. DECLASSIFICATION/DOWNGRADING SCHEDULE

16. DISTRIBUTION STATEMENT (of this Report)

Approved for public release, distribution unlimited

17. DISTRIBUTION STATEMENT (of the abstract entered in Block 20, if different from Report)

18. SUPPLEMENTARY NOTES

DDC RECEIVED JAN 11 1979 B

19. KEY WORDS (Continue on reverse side if necessary and identify by block number)

Surfaces, Polaritons, Silicon, Amplification

20. ABSTRACT (A theoretical investigation has been carried out on the effect of a drift current on surface polaritons in n-type silicon. The current direction is taken to be parallel to the direction of propagation of the surface polaritons. From the dispersion curves, there is evidence that an interaction takes place between the current and the polaritons which gives rise to polariton instability or amplification for certain frequency ranges. These instabilities are believed to be due to the presence of the surface.

DD 1 JAN 73 1473 EDITION OF 1 NOV 65 IS OBSOLETE

UNCLASSIFIED
SECURITY CLASSIFICATION OF THIS PAGE (When Data Entered)

403 659

78 12 11 155

AD A063097

DDC FILE COPY

THEORY OF SURFACE POLARITONS IN n-TYPE SILICON IN THE PRESENCE OF A DC CURRENT*

B. G. Martin†
Physics Department
University of California, Irvine
Irvine, California 92717
and
McDonnell Douglas Research Laboratories
McDonnell Douglas Corporation
St. Louis, Missouri 63166

and

A. A. Maradudin and R. F. Wallis
Physics Department
University of California, Irvine
Irvine, California 92717

Abstract

A theoretical investigation has been carried out on the effect of a drift current on surface polaritons in n-type silicon. The current direction is taken to be parallel to the direction of propagation of the surface polaritons. From the dispersion curves, there is evidence that an interaction takes place between the current and the polaritons which gives rise to polariton instability or amplification for certain frequency ranges. These instabilities are believed to be due to the presence of the surface.

* Work supported in part by the Office of Naval Research under Contract No. N00014-76-C-0121.

† Some of the results reported here are contained in a dissertation submitted in partial satisfaction of the requirements for a Ph.D. degree at the University of California at Irvine.

Technical Report No. 78-51

I. INTRODUCTION

Several theoretical investigations[1-5] have been made of the possibility of observing surface wave instabilities, e.g. amplifying surface waves, in a semiconductor due to drifting current carriers. The effect of a drift current on surface waves has also been observed experimentally[6,7]. In these studies, both electrons and holes were present in the semiconductor. In the present investigation, however, we restrict our attention to only one type of current carrier. We have theoretically investigated surface polaritons in n-type Si in the presence of drifting electrons. The primary objective of this investigation was to determine whether or not the surface polaritons exhibit instabilities due to the drifting electrons when only electrons and not holes are present.

II. SURFACE POLARITON DISPERSION RELATION

We begin by using non-local Maxwell's equations to obtain equations relating the field and dielectric tensor components. We next obtain an expression for the dielectric tensor, which is spatially dispersive. Imposing the so-called dielectric approximation, partially transformed components of the dielectric tensor are obtained. Using these results, the above-mentioned equations are solved for the field components, boundary conditions are applied, and the surface polariton dispersion relation is obtained.

Consider a semiconductor which is infinite in the x- and y-directions and semi-infinite in the z-direction. In seeking solutions to Maxwell's equations, we use the following form for the α^{th} Cartesian component of the electric field $\vec{E}$,

$$E_\alpha(\vec{x},t) = E_\alpha(z)e^{i(k_x x - \omega t)} \quad , \tag{2.1}$$

where k_x is the wave vector and ω is the frequency. Similar forms obtain for the displacement field $\vec{D}$ and magnetic field $\vec{H}$. In this paper we consider only surface polaritons with p-polarization, i.e., the electric vector lies in the sagittal plane defined by the direction of propagation and the normal to the surface. Consequently, $E_y = 0$, and if we eliminate the magnetic field from Maxwell's curl equations, the latter become

$$-\frac{d^2}{dz^2} E_x(z) + ik_x \frac{d}{dz} E_z(z) = \frac{\omega^2}{c^2} D_x(z) \tag{2.2a}$$

$$ik_x \frac{d}{dz} E_x(z) + k_x^2 E_z(z) = \frac{\omega^2}{c^2} D_z(z) \quad . \tag{2.2b}$$

A functional relationship is needed between $\vec{D}$ and $\vec{E}$ to complete the set of equations. For the crystal ($z \geq 0$), we can write

$$D_\alpha(z) = \sum_\beta \int_0^\infty dz' \, \epsilon_{\alpha\beta}(k_x\omega|zz')E_\beta(z') \quad . \tag{2.3}$$

Substituting Eq. (2.3) into Eqs. (2.2), we obtain the following pair of coupled integro-differential equations

$$-\frac{d^2}{dz^2} E_x(z) + ik_x \frac{d}{dz} E_z(z) = \frac{\omega^2}{c^2} \int_0^\infty dz' \epsilon_{xx}(k_x\omega|zz')E_x(z') + \frac{\omega^2}{c^2} \int_0^\infty dz' \epsilon_{xz}(k_x\omega|zz')E_z(z') \tag{2.4a}$$

$$ik_x \frac{d}{dz} E_x(z) + k_x^2 E_z(z) = \frac{\omega^2}{c^2} \int_0^\infty dz' \epsilon_{zx}(k_x\omega|zz') E_x(z')$$

$$+ \frac{\omega^2}{c^2} \int_0^\infty dz' \epsilon_{zz}(k_x\omega|zz') E_z(z') \qquad (2.4b)$$

which determine the field components $E_x(z)$ and $E_z(z)$.

In order to solve Eqs. (2.4) it is necessary to have expressions for the components of the dielectric tensor. We proceed by assuming that the motion of an average carrier in the semiconductor is governed by the transport equation[8],

$$[\dot{\vec{V}} + (\vec{V}\cdot\vec{\nabla})\vec{V}] = -\frac{\nabla P}{mN} + \frac{q}{m}[\vec{E} + \frac{1}{c}\vec{V} \times \vec{H}] - \nu\vec{V} \quad , \qquad (2.5)$$

where $\vec{V}$ and ν are the carrier velocity and collision frequency, respectively, $\vec{E}$ and $\vec{H}$ are the total electric and magnetic fields, respectively, m and N are the effective mass and particle density, respectively, and ∇P is the electron thermal pressure gradient. In what follows, the thermal pressure gradient is neglected, i.e., $\nabla P = 0$ (this is equivalent to neglecting the thermal motion of the current carriers).

We linearize Eq. (2.5) by writing $\vec{V} = \vec{V}_o + \vec{v}$, $\vec{E} = \vec{E}_o + \vec{e}$, $\vec{H} = \vec{H}_o + \vec{h}$, where $\vec{V}_o$, $\vec{H}_o$, and $\vec{E}_o$ are uniform and time-independent quantities while $\vec{v}$, $\vec{h}$, and $\vec{e}$ are position and time-dependent deviations from the uniform and static quantities. These linearized expressions are substituted into Eq. (1.1) and terms of like order on both sides are equated. We consider the situation where

$H_o = 0$. Nothing is obtained from the zero-order equation, but for the first-order equation we have

$$\dot{\vec{v}} + (\vec{V}_o \cdot \vec{\nabla})\vec{v} = \frac{q}{m}\vec{e} + \frac{q}{mc}(\vec{V}_o \times \vec{h}) - \nu\vec{v} \quad , \qquad (2.6)$$

where the dot indicates time-differentiation.

Assuming an exponential variation $\exp[i(\vec{k}\cdot\vec{r} - \omega t)]$ for the first-order quantities $\vec{v}$, $\vec{e}$, and $\vec{h}$, we can use the Maxwell equation $\vec{\nabla} \times \vec{e} = -\frac{1}{c}\dot{\vec{h}}$ to eliminate $\vec{h}$ from Eq. (2.10) and thus obtain the result

$$m[\omega\vec{v} + i\nu\vec{v} - (\vec{k}\cdot\vec{V}_o)\vec{v}] = iq[\vec{e} + \frac{1}{\omega}\vec{V}_o \times (\vec{k} \times \vec{e})] \quad . \qquad (2.7)$$

Solving this equation for $\vec{v}$ gives the result

$$\vec{v} = \vec{\vec{M}} \cdot \vec{e} \quad , \qquad (2.8)$$

where

$$\vec{\vec{M}} = \frac{iq}{a}\begin{pmatrix} \omega-(k_yV_{oy}+k_zV_{oz}) & k_xV_{oy} & k_xV_{oz} \\ k_yV_{ox} & \omega-(k_xV_{ox}+k_zV_{oz}) & k_yV_{oz} \\ k_zV_{ox} & k_zV_{oy} & \omega-(k_xV_{ox}+k_yV_{oy}) \end{pmatrix} \qquad (2.9)$$

and $a = m\omega(\omega - \vec{k}\cdot\vec{V}_o + i\nu)$.

The particle current is given by $\vec{G} = N\vec{V} = \vec{G}_o + \vec{g}$, where $\vec{G}_o = N_o\vec{V}_o$, $\vec{g} = N_o\vec{v} + n\vec{V}_o$, $N = N_o + n$, N_o is the mean particle density, and n is the deviation of the particle density from its mean value.

The equation of continuity can be written as

$$\dot{n} + \vec{\nabla}\cdot\vec{g} = 0 \quad , \qquad (2.10)$$

which, using the definition of $\vec{g}$ above, becomes

$$\dot{n} + \vec{V}_o \cdot \vec{\nabla} n + N_o(\vec{\nabla} \cdot \vec{v}) = 0 \quad . \tag{2.11}$$

The quantity n is a function of position and time which we express in the form $n(\vec{x},t) = n(\vec{k},\omega)\exp[i(\vec{k}\cdot\vec{r} - \omega t)]$. Substituting into Eq. (2.11) we find that

$$n = N_o \frac{\vec{k}\cdot\vec{v}}{\omega - \vec{k}\cdot\vec{V}_o} \quad . \tag{2.12}$$

Substituting this result into the equation for $\vec{g}$ above gives the result

$$\vec{g}(\vec{k},\omega) = N_o\left[\vec{v} + \frac{\vec{V}_o(\vec{k}\cdot\vec{v})}{\omega - \vec{k}\cdot\vec{V}_o}\right] \quad . \tag{2.13}$$

The electric current density can now be obtained from the relation

$$\vec{j} = q\vec{g} \quad . \tag{2.14}$$

In component form, this relation can be expressed as

$$j_\alpha(\vec{k},\omega) = \sum_\beta \sigma_{\alpha\beta}(\vec{k},\omega) e_\beta(\vec{k},\omega) \quad . \tag{2.15}$$

Using Eq. (2.8), we find that the nonlocal conductivity tensor $\sigma_{\alpha\beta}(\vec{k},\omega)$ is given by

$$\sigma_{\alpha\beta}(\vec{k},\omega) = N_o q\left[M_{\alpha\beta}(\vec{k},\omega) + \frac{V_{o\alpha}}{\omega - \vec{k}\cdot\vec{V}_o} \sum_\gamma k_\gamma M_{\gamma\beta}(\vec{k},\omega)\right] \quad . \tag{2.16}$$

The effective nonlocal dielectric tensor is related to the nonlocal conductivity tensor by

$$\epsilon_{\alpha\beta}(\vec{k},\omega) = \epsilon_\infty \delta_{\alpha\beta} + \frac{4\pi i}{\omega} \sigma_{\alpha\beta}(\vec{k},\omega) \tag{2.17}$$

where ϵ_∞ is the background dielectric constant. Note that the dielectric tensor is spatially dispersive due to the presence of terms containing the wave vector $\vec{k}$.

Before proceeding to obtain the surface polariton dispersion relation, a simplification will be made. Maradudin and Mills[9] have applied the so-called dielectric approximation to the type of dielectric tensor considered here. The simplification consists of assuming that this tensor depends on z and z′ only through their difference, as is the case for an infinitely extended medium. Surface corrections to the dielectric tensor are thus neglected. This is consistent with the assumption that the polariton decay length considered here is numerically large compared to the distance over which the dielectric constant varies near the surface.

For each of the dielectric tensor components obtained from Eq. (2.17), we need to evaluate the partially transformed dielectric tensor given by

$$\epsilon_{\alpha\beta}(k_x\omega|zz') = \int_{-\infty}^{\infty} \frac{dk_z}{2\pi}\, \epsilon_{\alpha\beta}(\vec{k},\omega) e^{ik_z(z-z')} \quad , \qquad (2.18)$$

where we have taken $k_y = V_{oy} = V_{oz} = 0$. The results are

$$\epsilon_{xx}(k_x\omega|zz') = (\epsilon_\infty - \frac{\beta_2}{\beta_1})\delta(z-z') + \frac{\beta_3}{\beta_1} \frac{\partial^2\delta(z-z')}{\partial z^2} \qquad (2.19a)$$

$$\epsilon_{xz}(k_x\omega|zz') = -i\beta_4 \frac{\partial\delta(z-z')}{\partial z'} = \epsilon_{zx}(k_x\omega|zz') \qquad (2.19b)$$

$$\epsilon_{zz}(k_x\omega|zz') = (\epsilon_\infty - \beta_5)\delta(z-z') \quad , \qquad (2.19c)$$

where $\delta(z-z')$ is the Dirac delta function, and where we have used the definitions

$$\beta_1 = m^2\omega^2(\omega - k_x V_{ox})(\omega - k_x V_{ox} + i\nu)^2 \qquad (2.20a)$$

$$\beta_2 = \epsilon_\infty m^2 \omega^2 \omega_p^2 (\omega - k_x V_{ox} + i\nu) \qquad (2.20b)$$

$$\beta_3 = \epsilon_\infty m^2 \omega_p^2 V_{ox}^2 (\omega - k_x V_{ox} + i\nu) \qquad (2.20c)$$

$$\beta_4 = \frac{\epsilon_\infty \omega_p^2 V_{ox}}{\omega^2(\omega - k_x V_{ox} + i\nu)} \qquad (2.20d)$$

$$\beta_5 = \frac{\epsilon_\infty \omega_p^2}{\omega^2} \frac{(\omega - k_x V_{ox})}{(\omega - k_x V_{ox} + i\nu)} \quad , \qquad (2.20e)$$

and $\omega_p^2 = 4\pi N_o q^2/m\epsilon_\infty$.

The integrations in Eqs. (2.4) can now be carried out, with the result that we are left with the coupled differential equations:

$$\frac{-d^2E_x(z)}{dz^2} + ik_x \frac{dE_z(z)}{dz} = \frac{\omega^2}{c^2}\left(\epsilon_\infty - \frac{\beta_2}{\beta_1}\right) E_x(z) + \frac{\beta_3}{\beta_1}\frac{\omega^2}{c^2} \frac{d^2E_x(z)}{dz^2} + \\ + i\frac{\omega^2}{c^2}\beta_4 \frac{dE_z(z)}{dz} \qquad (2.21a)$$

$$ik_x \frac{dE_x(z)}{dz} + k_x^2 E_z(z) = i\frac{\omega^2}{c^2}\beta_4 \frac{dE_x(z)}{dz} + \frac{\omega^2}{c^2}(\epsilon_\infty - \beta_5)E_z(z) \quad . \qquad (2.21b)$$

It is assumed that for the crystal ($z \geq 0$),

$$E_x(z) = Ce^{-\alpha z}, \quad E_z(z) = De^{-\alpha z} \quad , \qquad (2.22)$$

where C and D are constants. Substituting these expressions into the coupled differential equations gives us two equations relating C and D. Setting the determinant of the coefficients of C and D equal to zero gives us an expression for the decay constant α:

$$\alpha^2 = \frac{\left(\epsilon_\infty - \frac{\beta_2}{\beta_1}\right)\left[k_x^2 - \frac{\omega^2}{c^2}(\epsilon_\infty - \beta_5)\right]}{\epsilon_\infty - \frac{\beta_3}{\beta_1}\left(k_x^2 - \epsilon_\infty \frac{\omega^2}{c^2}\right) - \beta_5 - 2k_x\beta_4} \quad . \tag{2.23}$$

From Eq. (2.21b) we obtain the following relation between C and D:

$$D = C \frac{i\alpha\left(k_x - \frac{\omega^2}{c^2}\beta_4\right)}{k_x^2 - \frac{\omega^2}{c^2}(\epsilon_\infty - \beta_5)} \quad . \tag{2.24}$$

Another field component needed is $D_z(z)$; from Eq. (2.3) and using Eqs. (2.19) we obtain

$$D_z(z) = i\beta_4 \frac{dE_x(z)}{dz} + (\epsilon_\infty - \beta_5)E_z(z) \quad . \tag{2.25}$$

Consider next the electric fields in the vacuum ($z < 0$) where $D_\alpha(z) = E_\alpha(z)$. Assuming that

$$E_x(z) = Ae^{\alpha_o z}, \quad E_z(z) = B\, e^{\alpha_o z} \quad , \tag{2.26}$$

and proceeding as for the case of the crystal, one obtains the following results for the decay constant

$$\alpha_o^2 = k_x^2 - \frac{\omega^2}{c^2} \tag{2.27}$$

and the relation between A and B

$$B = -\frac{ik_x}{\alpha_o} A \quad . \tag{2.28}$$

The boundary conditions at $z = 0$ can now be applied. Continuity of $E_x(z)$ gives the result $C = A$, while the continuity of $D_z(z)$ produces

$$-\frac{ik_x}{\alpha_o} A = -i\beta_4 \alpha C + i\alpha C \frac{(\epsilon_\infty - \beta_5)(k_x - \frac{\omega^2}{c^2}\beta_4)}{k_x^2 - \frac{\omega^2}{c^2}(\epsilon_\infty - \beta_5)} \quad , \tag{2.29}$$

from which we obtain the surface polariton dispersion relation

$$\frac{1}{\alpha\alpha_o} + \frac{\epsilon_\infty - \beta_5 - k_x\beta_4}{k_x^2 - \frac{\omega^2}{c^2}(\epsilon_\infty - \beta_5)} = 0 \quad . \tag{2.30}$$

III. RESULTS AND DISCUSSION

Theoretical dispersion curves have been obtained for surface polaritons in the presence of drifting current carriers. The effect of retardation is included, but the effect of damping due to scattering of the carriers is neglected. The latter assumption is reasonable in high mobility material.

Calculations were made using values of parameters appropriate for n-type Si. The value of the background dielectric constant ϵ_∞ was taken to be 11.7. The density-of-states effective mass $m^* = (m_\ell^* m_t^{*2})^{1/3}$ used in the calculations was obtained from the values[10] $m_t^* = 0.19 m_o$ and $m_\ell^* = 0.98\ m_o$. The electron mobility μ_e was taken to be[11] 1.6×10^3 cm^2/V sec.

In our calculations, the thermal pressure gradient was neglected (see Eq. (1.1). This is valid if the following inequality holds[3]:

$$\frac{\omega}{\nu} \frac{V_F}{V_{ox}} < 1 \quad , \tag{3.1}$$

where $\nu = e/m^*\mu_e$ is the damping constant and $V_F = (\hbar/m^*)(3\pi^2 N_o)^{1/3}$ is the Fermi velocity. The practical upper limit for the election drift velocity V_{ox} is $\sim 10^8$ cm/sec, which corresponds to an electric

field of $\sim 10^5$ volts/cm, obtained from the equation $V_{ox} = E_{ox}\mu_e$, where the value of μ_e is as given above. For n-type Si, it has been shown that the mobility of the electrons doesn't vary with electric field up to 10^5 volts/cm[12]. Three values of drift velocity were considered: $V_{ox} = 0.0001c$, $0.001c$, and $0.01c$.

For the parameter values given here for n-type Si, an upper limit for the carrier concentration N_o can be calculated from Eq. (3.1). Taking $V_{ox} = 0.0001c$ and $\omega \cong \omega_p = (4\pi N_o e^2/m^*\epsilon_\infty)^{\frac{1}{2}}$, we obtain the result $N_o \lesssim 4 \times 10^{18} cm^{-3}$.

In making the calculations of the dispersion curves, real values of ω/ω_p were assumed, and complex values of the wave vector $k_x = k_1 + ik_2$ and the decay constant $\alpha = \alpha_1 + i\alpha_2$ were calculated using a digital computer. The values of ω/ω_p were taken in steps of 0.01 or smaller for the range $0 < \omega/\omega_p < 1.0$. The values of k_x were calculated using Muller's method[13], a process of successive approximations from initial guesses (which need not be externally supplied).

Figures 1 and 2 show the dispersion curves for the situation where the drift velocity $V_{ox} = 0.0001c$. Note that for $k_1 > 0$, there is one branch, which for $\omega \lesssim 0.5\ \omega_p$, follows the light line; then, for higher frequencies it bends over and moves to the right of the light line. For frequencies $\omega \lesssim 0.95\ \omega_p$, there are three branches for $k_1 < 0$ in Fig. 2 which will be termed negative branches in the discussion that follows. Two of the three negative branches occur because of the presence of the drift velocity; for if $V_{ox} = 0$, there is only one negative branch, a mirror image of the positive branch with $k_1 > 0$.

At the lower frequencies, two of the negative branches (branches a and b in Fig. 2) have large values for $|ck_1/\omega_p|$ which decrease as the frequency increases. The other negative branch (branch c in Fig. 2) originates at the origin and increases in frequency as $|k_1|$ increases. Eventually, a point is reached where branch c intersects branch a. To the right of this intersection point, there exists a continuation of branch a indicated by the dash-dot lines in Figs. 1 and 2, which consists of two degenerate modes whose wave vectors form a complex conjugate pair. As the frequency increases above the value at the intersection point, this degenerate mode moves to the right and finally terminates at the vertical axis at $\omega = \omega_p$. In addition, the real part of the decay constant α becomes zero at the termination point.

The remaining negative branch in Fig. 2 (branch b) also moves in closer to the light line as the frequency increases, and then terminates at a point where the frequency is slightly below ω_p. At this end point, the decay constant α becomes pure imaginary, i.e., we no longer meet the condition for surface polaritons. We note also that branch b intersects branch a at a large value of $|ck_1/\omega_p|$.

As we see from Figs. 1 and 2, there is a frequency range where we have a degenerate negative branch whose wave vectors form a complex conjugate pair. For all the other negative branches, the wave vectors are real except in the immediate vicinity of the point where branches a and b intersect. A plot of the magnitude of the imaginary part of the reduced wave

vector $|ck_2/\omega_p|$, versus frequency is shown in Fig. 3 for the degenerate pairs. The curves for $|ck_2/\omega_p|$ start at $k_2 = 0$ for $\omega \simeq 0.96\ \omega_p$, rapidly increase with increasing frequency to a maximum, then reverse and approach $k_2 = 0$ again as ω approaches ω_p. In addition, k_2 is non-zero over a very narrow frequency range about $\omega = 0.92\ \omega_p$ where branches a and b intersect in Fig. 2.

Figure 4 shows the frequency dependence of the real part of the reduced decay constant, $c\alpha_1/\omega_p$, versus frequency for V_{ox}=0.0001 c. The branches are labelled to correspond to Fig. 2. For that frequency range where the wave vector is complex conjugate (see Fig. 2), the decay constant is also complex conjugate.

Figure 5 shows the dispersion curves for an order of magnitude higher drift velocity, i.e., $V_{ox} = 0.001$ c, in a region of negative k_1. For our purposes, the region of interest centers on the point where branches a and c intersect. Again, we have complex conjugate values of k_x in the upper of the intersecting branches to the right of the intersection point. There is, as was the case for $V_{ox} = 0.0001$ c considered previously, a positive branch, which although not shown, is essentially the same as that shown in Fig. 1. We also have complex values of k_1 in the immediate vicinity of the intersection point of branches a and b.

Figure 5 differs from Fig. 2 in two noticeable ways: in Fig. 5, the intersection point of branches a and c occurs at a smaller value of $|k_1|$ than in Fig. 2, and the uppermost negative branch (branch b) moves to a smaller value of $|k_1|$ before terminating. As before, the termination point occurs when the decay constant no longer satisfies the requirement $\mathrm{Re}\alpha > 0$. In addition, the point of intersection of branches a and b occurs at a much smaller value of $|k_1|$ than in Fig. 2.

In Fig. 6, the frequency dependence of the imaginary part of the surface polariton wave vector for $V_{ox} = 0.001$ c is presented It shows a behavior somewhat different from that shown in Fig. 3, the case for $V_{ox} = 0.0001c$. The frequency range where complex conjugate wave vectors occur is larger for the higher drift velocity, while the maximum value of $|ck_2/\omega_p|$ is smaller.

Figure 7 shows dispersion curves for the highest drift velocity considered here, namely $V_{ox} = 0.01c$. The relative behavioral changes discussed in the last two paragraphs continue for $V_{ox} = 0.01c$, except for one obvious difference: branches a and b now coincide over an appreciable frequency range, the wave vectors in this range being complex conjugates of one another. As the frequency increases, the branches separate, the lower one finally intersecting branch c in the same manner as shown in Figs. 2 and 5. The intersection point differs from those of Figs. 2 and 5 in that it occurs at a smaller value of $|k_1|$. In addition, branch b in Fig. 7 moves to a smaller value of $|k_1|$ before terminating than is the case in Figs. 2 and 5. The plot of $|ck_2/\omega_p|$ vs. ω is shown in Fig. 8 for $V_{ox} = 0.01c$. Note from Figs. 3, 6, and 8 that the frequency range where complex conjugate wave vectors occur is larger, the higher the drift velocity, while the maximum value of $|ck_2/\omega_p|$ is smaller.

We now consider in detail the degenerate modes whose wave vectors form a complex conjugate pair. One of these modes has the imaginary part of the wave vector negative, so that the amplitude increases as the mode propagates. We therefore have

an apparent instability. This instability may be caused by the presence of the surface. Specifically, the important factor leading to the instability may be the large electron density gradient that occurs in the vicinity of the crystal surface.

So-called convection and nonconvection instabilities occur in plasmas[15,16] and are labeled according to whether or not the signs of the group velocities ($d\omega/dk_x$) of the interacting modes are the same prior to switching on the interaction. If the group velocities have the same sign, then the interaction can result in a convective instability.which may be interpreted as an amplifying wave. If, however, the group velocities have opposite signs, the interaction can result in a nonconvective instability where certain real wave vectors correspond to complex frequencies or in an evanescent wave where certain real frequencies correspond to complex wave vectors.

For the interaction associated with the intersection of branches a and c, we shall regard the unperturbed modes to be the surface polaritons and the electron drift current. The latter is taken to have a positive drift velocity (group velocity), whereas the former has a negative group velocity. Since the two group velocities are of opposite sign, we expect that there may be either an evanescent wave or a nonconvective instability. Our calculations show that tht degenerate branch under discussion occurs in a range of real frequencies with complex wave vectors. Consequently, the growing wave of this degenerate branch is an evanescent wave.

We now turn to the second type of interaction which is associated with the intersection of branches a and b. In this case the two group velocities of the interacting modes have the same sign. As already stated, this branch involves a range of real frequencies with complex wave vectors. We have also verified that if we choose the wave vector real, the frequencies for the degenerate branch are complex. The growing wave in this second type of degenerate branch is therefore an amplifying wave and corresponds to a convective instability. It should also be emphasized that the instabilities reported in this paper occur in the presence of only one type of current carrier and do not require two types of current carriers such as electrons and holes.

In a recent paper,[16] Tajima and Ushioda have presented theoretical results on surface polaritons in polar semiconductors in the presence of a current. Under certain circumstances, they find instabilities associated with the coupling of surface plasmons with surface optical phonons, but do not report instabilities of the type discussed in the present paper. Tajima and Ushioda used a different method of handling spatial dispersion than the present authors and did not investigate negative values of the wave vector, so it is not surprising that they did not observe the instabilities reported here.

IV. REFERENCES

1. G. A. Baraff and S. J. Buchsbaum, Appl. Phys. Lett. 6 (1965) 219.
2. G. A. Baraff and S. J. Buchsbaum, IEEE Trans. Electron Devices ED-13 (1966) 203.
3. G. A. Baraff and S. J. Buchsbaum, Phys. Rev. 144 (1966) 266.
4. G. S. Kino, Appl. Phys. Lett. 12 (1968) 312.
5. A. Bers and B. E. Burke, Appl. Phys. Lett. 16 (1970) 300.
6. B. E. Burke and G. S. Kino, Appl. Phys. Lett. 12 (1968) 310.
7. C. Krischer and A. Bers, Appl. Phys. Lett 18 (1971) 349.
8. L. Spitzer, Physics of Fully Ionized Gases (Interscience Publishers, Inc., New York, 1962).
9. A. A. Maradudin and D. L. Mills, Phys. Rev. B7 (1973) 2787.
10. R. N. Dexter et al., Phys. Rev. 96 (1954) 220.
11. C. Kittel, Introduction to Solid State Physics, 3rd Ed. (John Wiley, New York, 1968), p. 308.
12. A. C. Prior, J. Phys. Chem. Solids 12 (1960) 175.
13. D. E. Muller, Math. Tab. Wash. 10 (1956) 208.
14. N. Rostoker, private communication.
15. P. A. Sturrock, Phys. Rev. 112 (1958) 1488.
16. T. Tajima and S. Ushioda, Phys. Rev. B18 (1978) 1892.

FIGURE CAPTIONS

Fig. 1. Dispersion curves for surface polaritons in n-type Si ($V_{ox}/c = 0.0001$).

Fig. 2. Dispersion curves for surface polaritons in n-type Si ($V_{ox}/c = 0.0001$).

Fig. 3. The frequency dependence of the imaginary part of the wave vector associated with surface polaritons in n-type Si ($V_{ox}/c = 0.0001$)

Fig. 4. The frequency dependence of the real part of the decay constant associated with surface polaritons in n-type Si ($V_{ox}/c = 0.0001$).

Fig. 5. Dispersion curves for surface polaritons in n-type Si ($V_{ox}/c = 0.001$).

Fig. 6. The frequency dependence of the imaginary part of the wave vector associated with surface polaritons in n-type Si ($V_{ox}/c = 0.001$).

Fig. 7. Dispersion curves for surface polaritons in n-type Si ($V_{ox}/c = 0.01$).

Fig. 8. The frequency dependence of the imaginary part of the wave vector associated with surface polaritons in n-type Si ($V_{ox}/c = 0.01$).

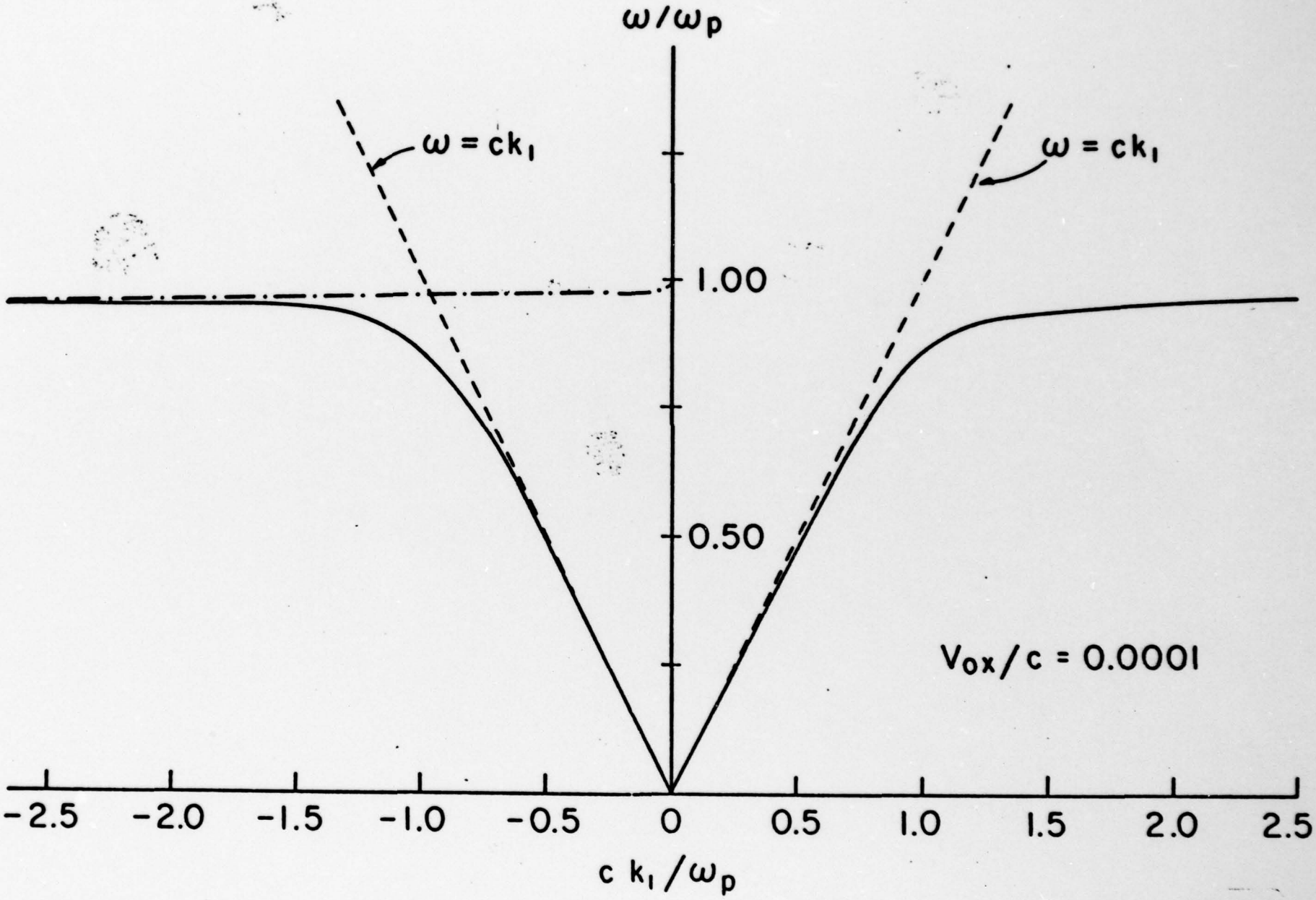
ω/ωp
ω = ck1
ω = ck1
1.00
0.50
Vox/c = 0.0001
-2.5
-2.0
-1.5
-1.0
-0.5
0
0.5
1.0
1.5
2.0
2.5
c k1/ωp

Fig. 1

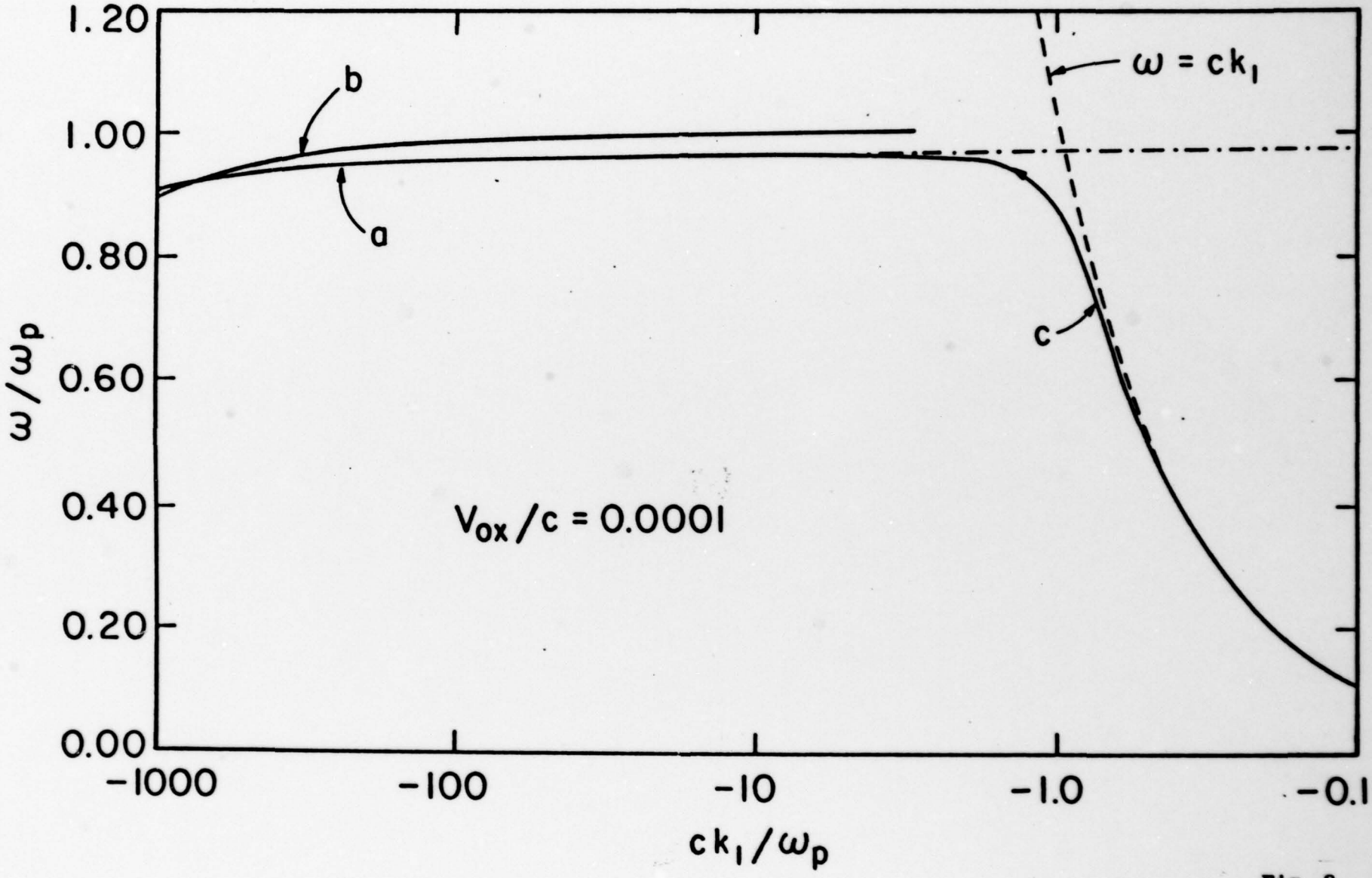
1.20
1.00
0.80
0.60
0.40
0.20
0.00
ω/ωp
b
a
c
ω = ck1
Vox/c = 0.0001
-1000
-100
-10
-1.0
-0.1
ck1/ωp

Fig. 2

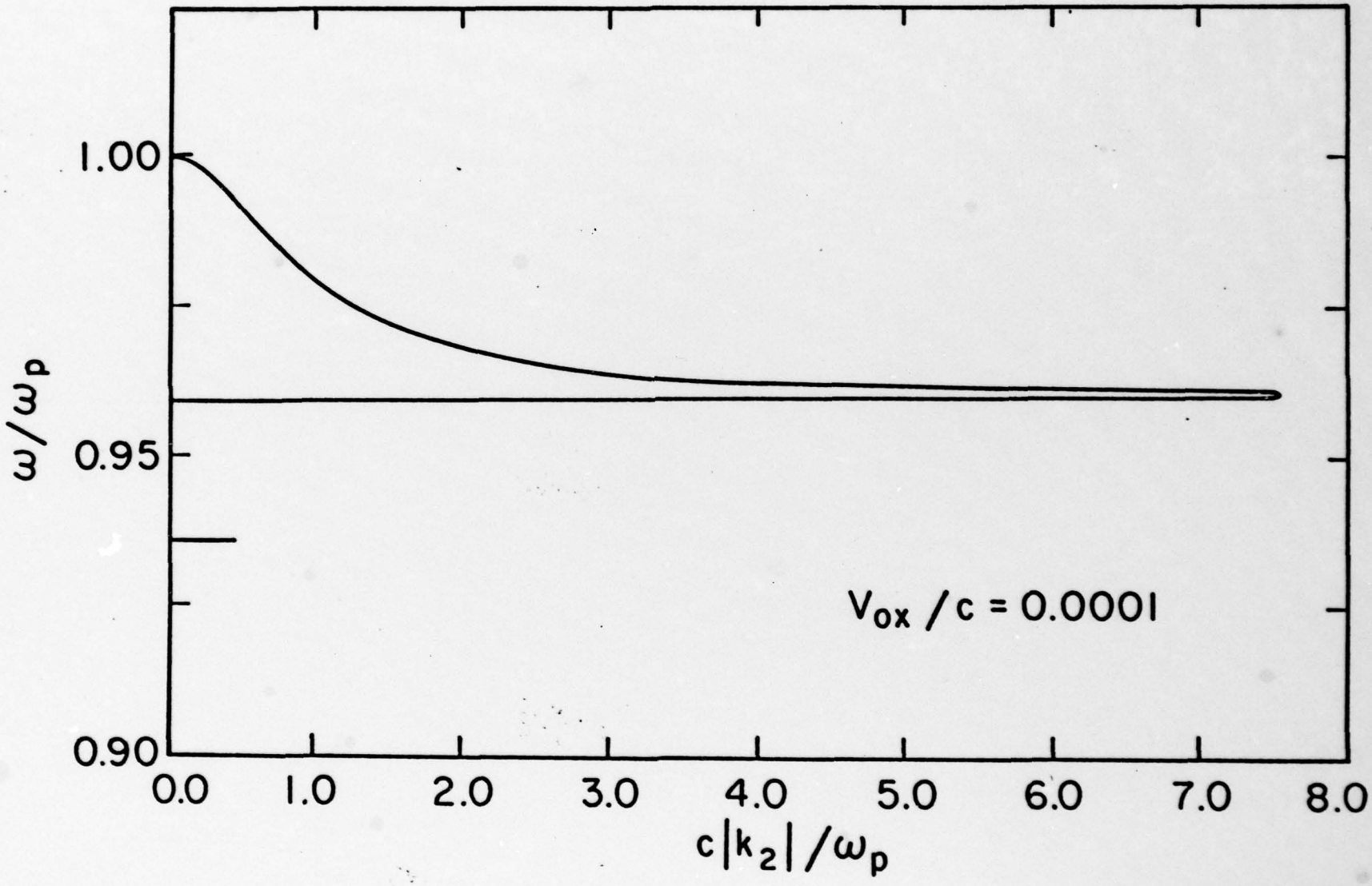

Fig. 3

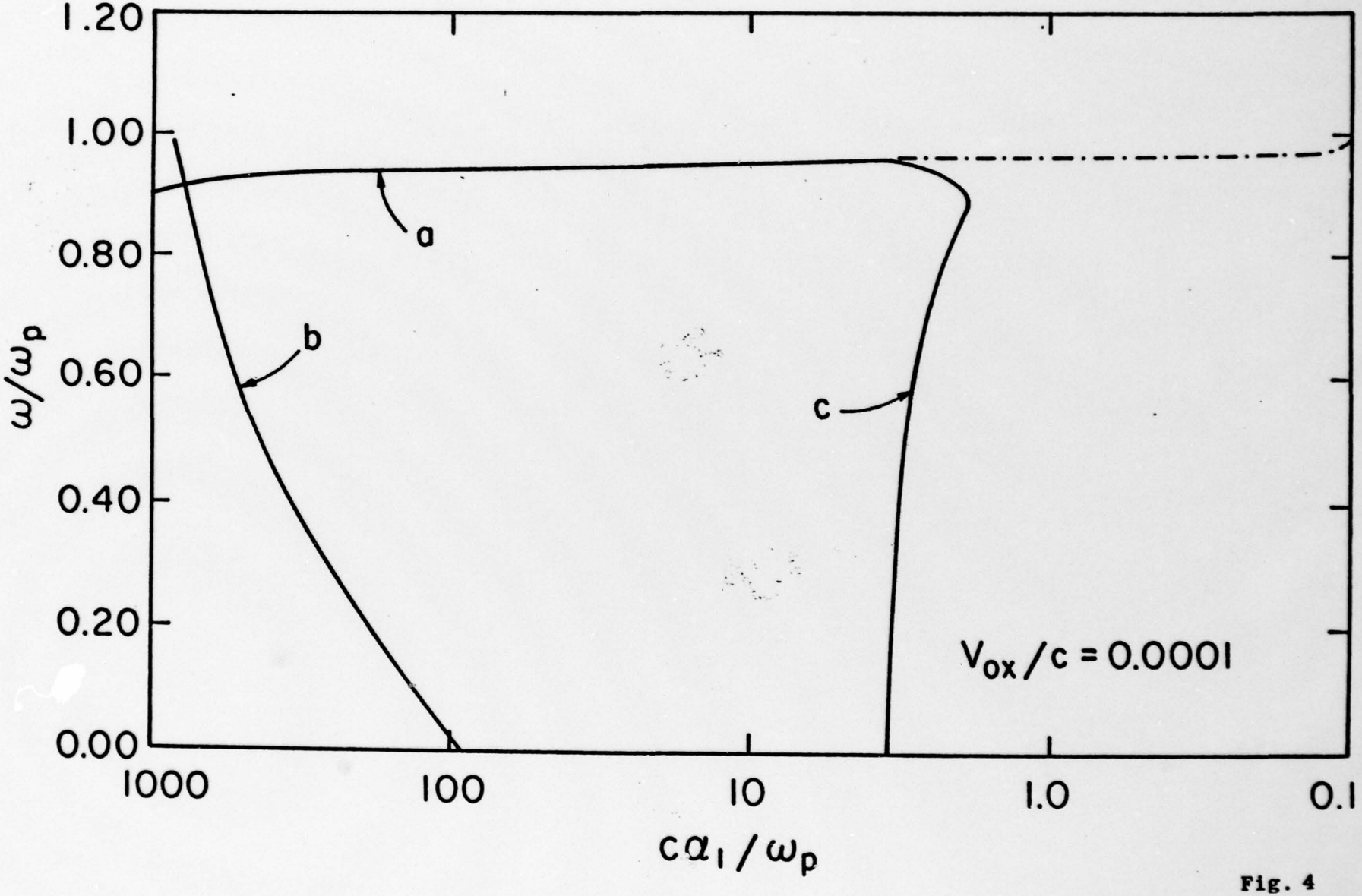
1.20
1.00
0.80
0.60
0.40
0.20
0.00
ω/ωp
a
b
c
Vox/c = 0.0001
1000
100
10
1.0
0.1
cα1/ωp

Fig. 4

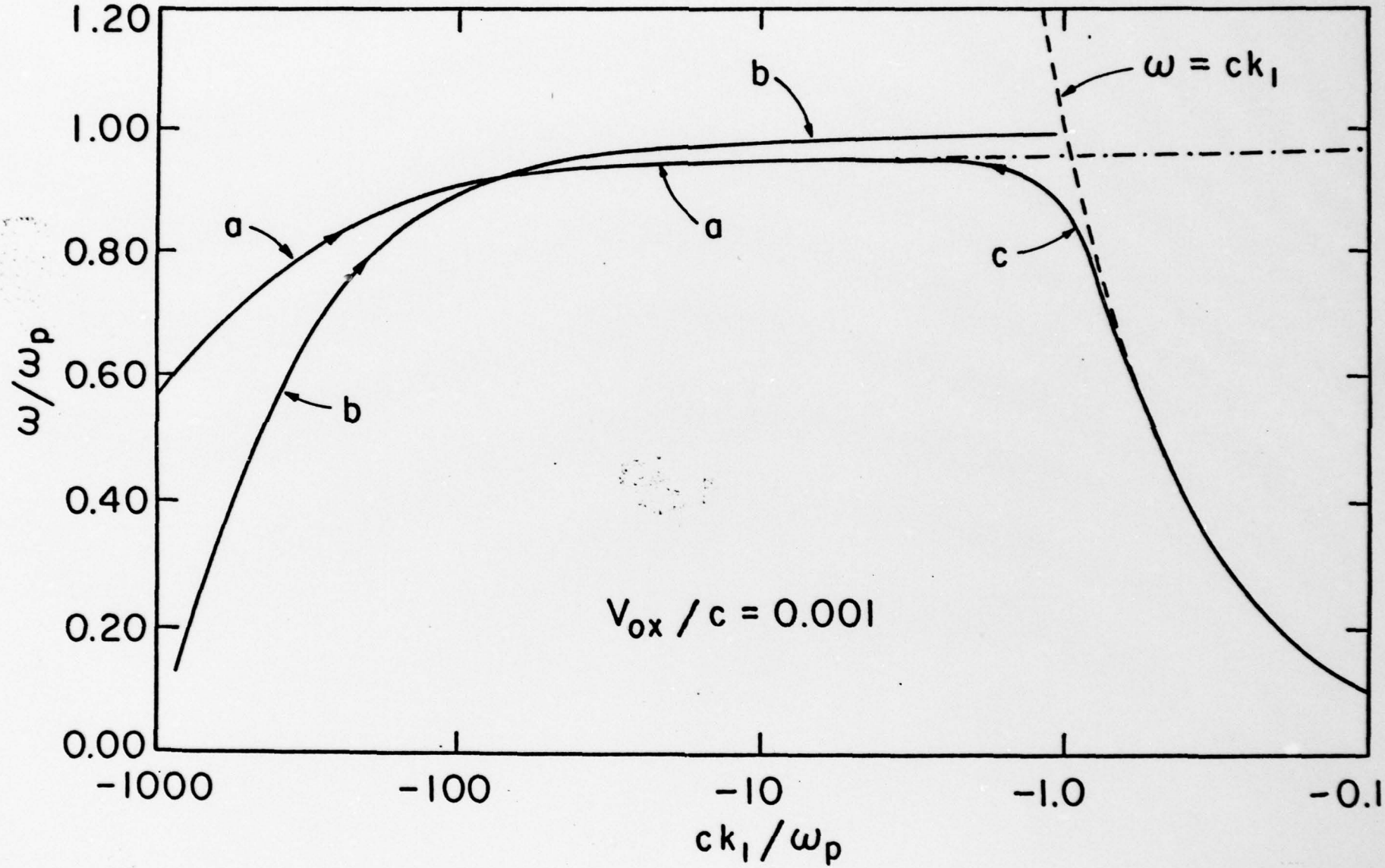
1.20
1.00
0.80
0.60
0.40
0.20
0.00
ω/ωp
-1000
-100
-10
-1.0
-0.1
ck1/ωp
ω = ck1
a
b
c
Vox / c = 0.001

Fig. 5

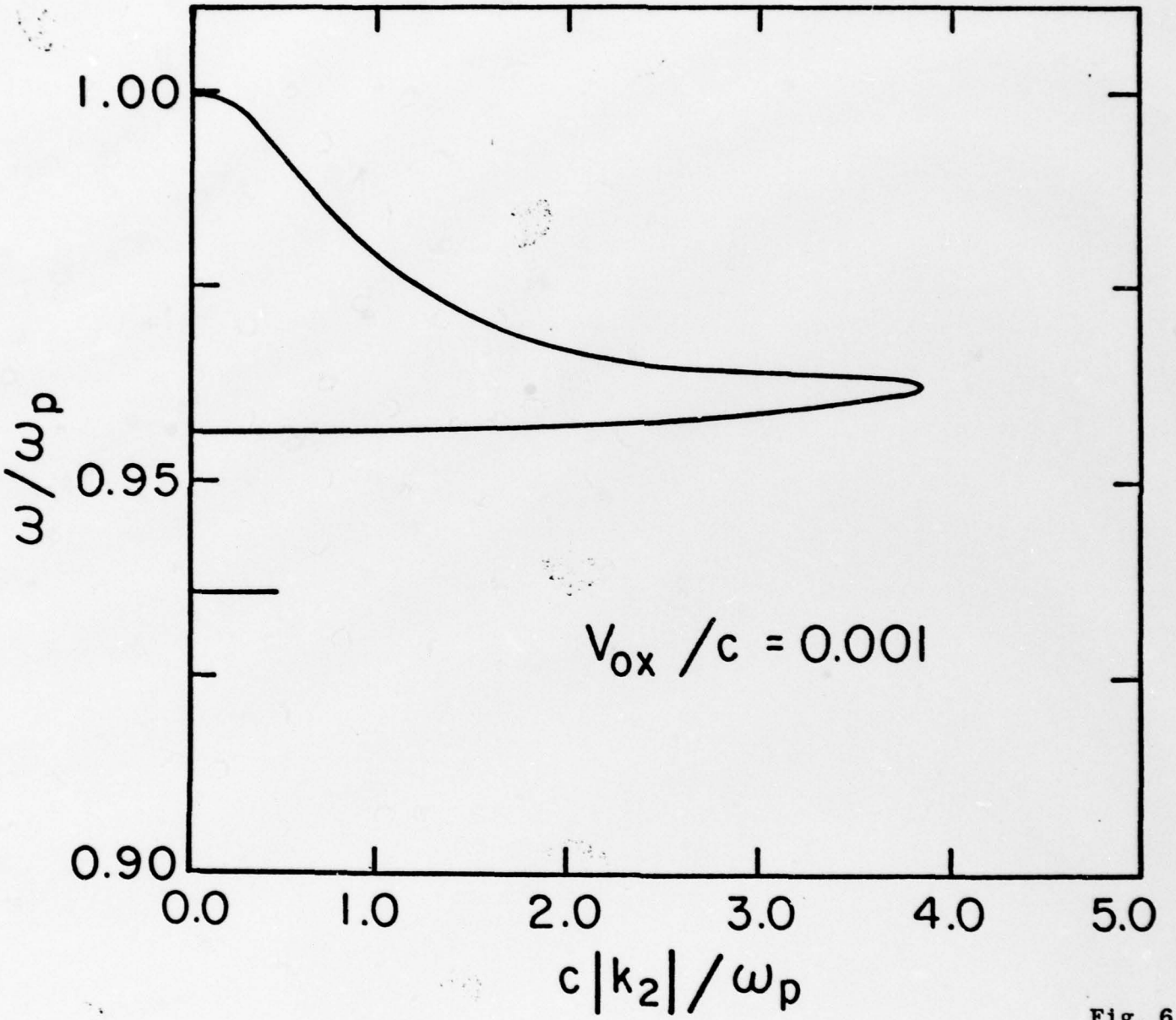

Fig. 6

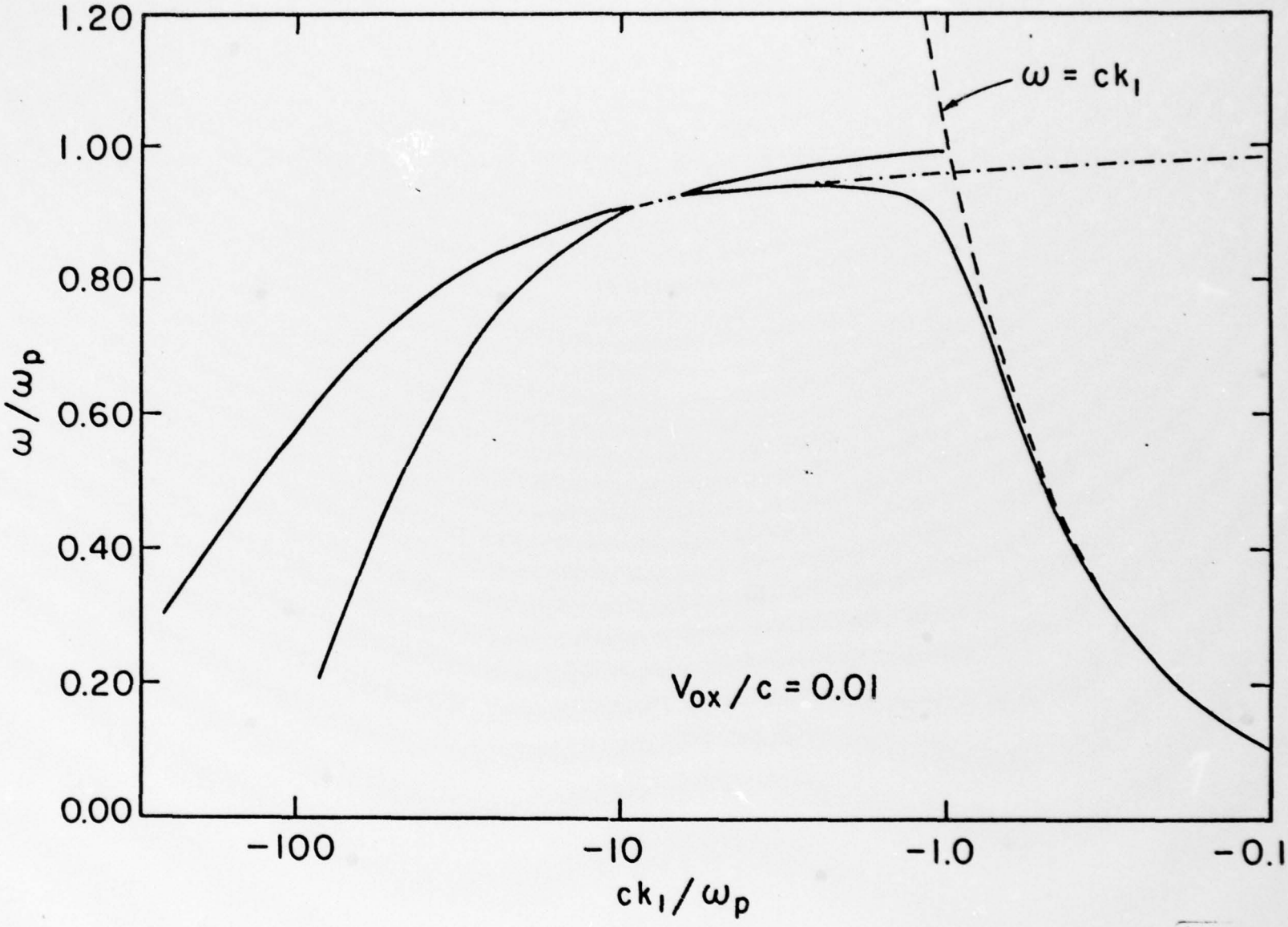

Fig. 7

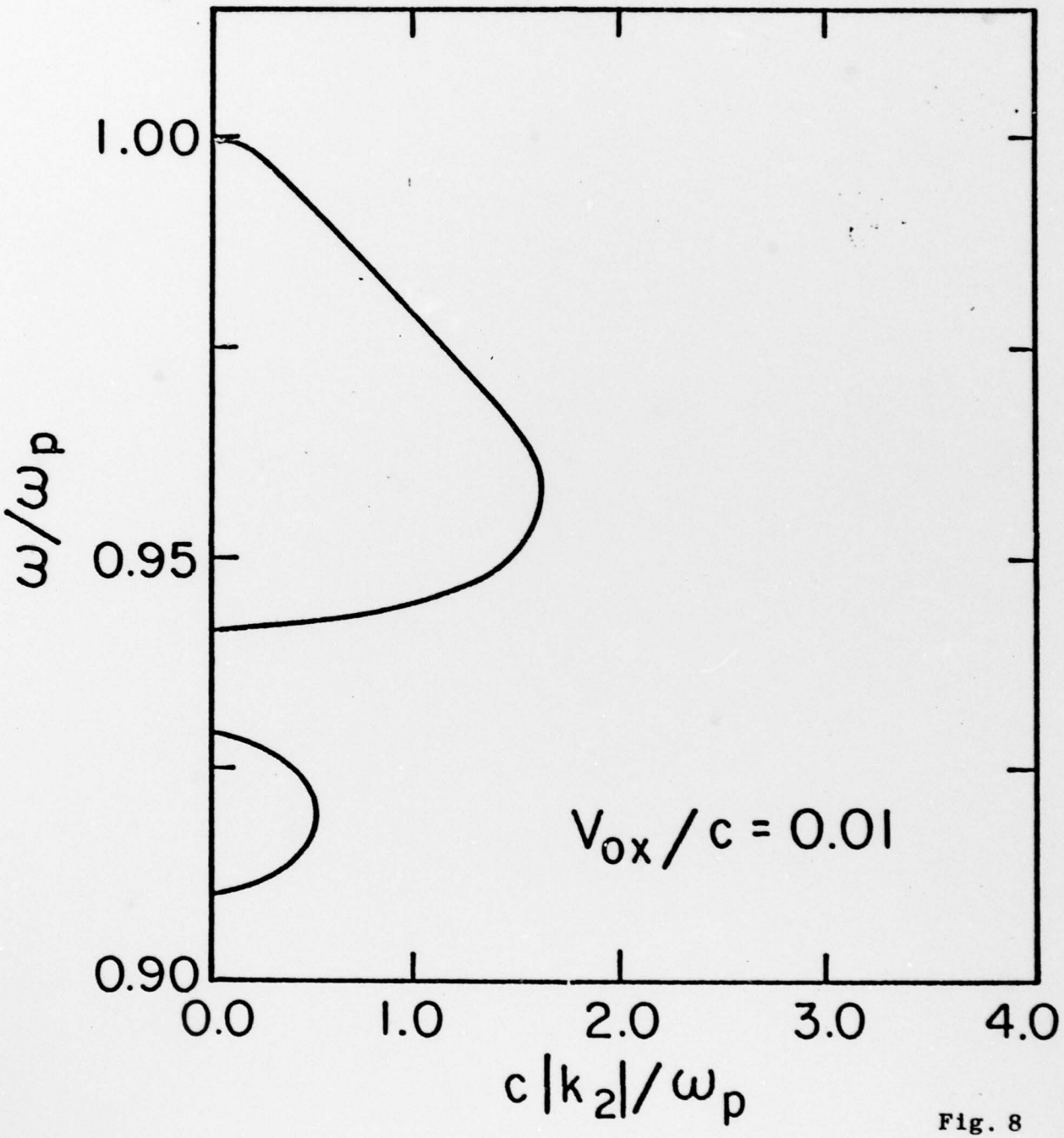

Fig. 8